

Simulating smoke movement through long vertical shafts in zone-type compartment fire models

Leonard Y. Cooper

*Building and Fire Research Laboratory, National Institute of Standards and Technology,
Gaithersburg, MD 20899, USA*

Received 7 January 1997; revised version received 15 October 1997; accepted 20 November 1997

Abstract

A limitation of traditional zone-type compartment fire modeling is the inadequacy of two-layer quasi-steady-buoyant-plume analyses to simulate the fire-generated environment in room configurations with large height-to-span ratios, e.g., elevator shafts and ventilation shafts. Model equations to remove this limitation are developed. These simulate time-dependent flow in a long, ventilated, vertical shaft with an arbitrary vertical density distribution, including one or more intervals along the shaft length where the vertical distribution of the averaged cross-section density may be unstably stratified, i.e., density increasing with increasing elevation. The model equations are partially verified by favorable comparisons between solutions and previously published data from unsteady experiments in long vertical tubes involving initially unstable configurations: saltwater over freshwater and heavy gas over light gas. Published by Elsevier Science Ltd.

Notation

C_p	Specific heat at constant pressure
c_{BOT}, c_{TOP}	Concentrations of top, bottom fluids
d	Characteristic span of a room or section of a shaft, e.g., diameter
D	Eddy diffusivity
g	Acceleration of gravity
k	Thermal conductivity
K	Constant, Eq. (11)
K_G, K_{BR}	Eqs. (13) and (14)
l	Characteristic length of the fluid mixing process

L	Characteristic height of the compartment space, e.g., length of shaft
\dot{m}'''_{VENT}	Rate of mass added to the shaft per unit volume
\dot{q}'''_{HT}	Rate of heat transferred to the gas in the shaft per unit volume
Q	Volume flow rate
t	Time
t_{ARRIVAL}	t when $z_{\text{FRONT}} = L$
T	Temperature in the shaft averaged across the section
T_{VENT}	Temperature of gas flowing through a vent and into the shaft
\bar{T}	Time-averaged component of T
T'	Fluctuating component of T
V_z	Flow velocity in the z direction averaged across a section
\bar{V}_z	Time-averaged component of V_z
V'_z	Fluctuating component of V_z
w'	Characteristic velocity of the turbulent fluctuations
z	Coordinate in upward direction
z_{FRONT}	z of diffusion front

Greek letters

Γ	Eq. (23)
$\Delta\rho$	$\rho_{\text{TOP}} - \rho_{\text{BOT}}$
ε	Eq. (17)
ζ	Eq. (17)
ζ_{FRONT}	ζ at the diffusion front
η	Eq. (18)
η_{FRONT}	η at $\zeta = \zeta_{\text{FRONT}}$
θ	Eq. (17)
ρ	density averaged across the section
$\rho_{\text{AMB}}, \rho_{\text{VENT}}$	ρ of ambient, gas flowing through a vent and into the shaft
$\bar{\rho}$	Time-averaged component of ρ
ρ'	Fluctuating component of ρ
ρ_{AVE}	$(\rho_{\text{TOP}} + \rho_{\text{BOT}})/2$
$\rho_{\text{TOP}}, \rho_{\text{BOT}}$	ρ of fluid in top, bottom of the vessels; initial ρ at top, bottom of shaft
$\tau, \tau_{\text{ARRIVAL}}$	Eqs. (17) and (26)
ϕ	Eq. (23)
ψ	Eqs. (23) and (24)
ω	Dummy variable, Eq. (24)
Ω	Eq. (29)

1. Introduction

1.1. A limitation of the two-layer zone-type modeling approach for shaft-like 'rooms'

The traditional, zone-type, compartment-fire-modeling strategy, which uses the concepts of one-to-two uniform layers per room, room-to-room mass exchanges by

vent flows, and layer-to-layer mass exchange by quasi-steady buoyant plumes, has proven to be very robust. However, these basic concepts are inadequate for long, vertical shaft-like 'rooms'.

Let L and d , be the characteristic height and horizontal span, respectively, of a room configuration. Then, for rooms with $L/d \gg 1$ (shafts or ducts) it is not reasonable to expect a traditional, two-layer, zone-type, fire modeling approach to lead to a successful simulation of fire environments. For such room configurations, some of the basic modeling assumptions become invalid. Thus, (1) as the plume rises and spreads, its volume eventually becomes significant and it starts to fill a large fraction of the section of the shaft/duct, (2) it is not reasonable to expect that characteristic times of mixing in the shaft will generally be small compared to characteristic times of interest, and (3) there is no basis for a uniform, two-layer approximation to the density/temperature distribution.

An illustration of a generic problematic facility and room configuration is presented in Fig. 1. In the facility shown, traditional modeling concepts would typically be

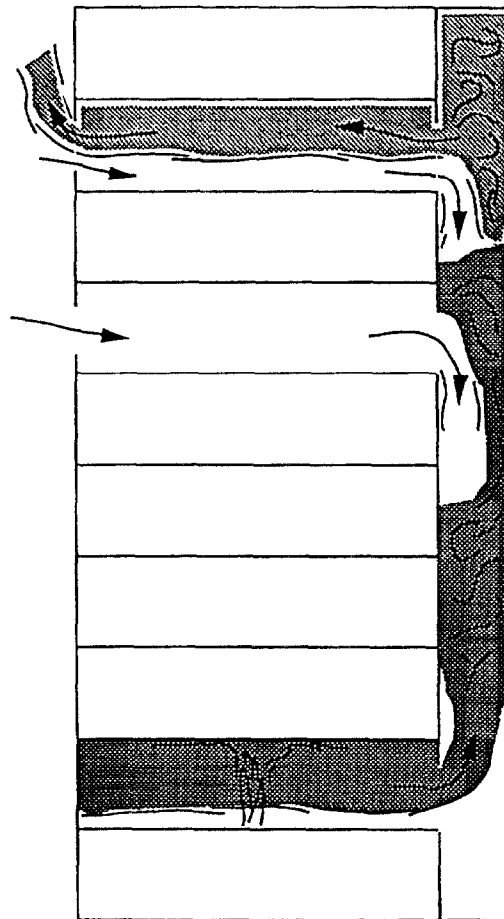


Fig. 1. Sketch of a facility where traditional, two-layer, zone-type, modeling concepts are not uniformly applicable.

applicable in the small- L/d rooms of fire origin, the upper floors, etc., but they would not be applicable in the large- L/d shaft.

1.2. A strategy for modeling flow through shaft-like spaces in zone-type compartment fire models; objective of this work

For the traditional two-layer, etc., zone-type modeling approach to be valid, large- L/d spaces in a multi-room facility need to be treated as a special class of room configuration. Fire-generated environments there need to be simulated with a method of analysis that (1) uses a valid intra-room fire dynamics modeling approach and (2) can be implemented in the compartment fire model to study fire scenarios in facilities which include other 'standard', i.e., small-to-moderate- L/d , room elements. The purpose of this paper is to develop a framework for such an analysis.

Once a method of analyzing large- L/d spaces is developed and verified, it could be incorporated into an existing multi-room fire model. The revised model would then be capable of describing smoke movement through shaft-like spaces that may be included in the design of a particular facility of interest. The strategy for carrying out simulations with the revised fire model would involve categorizing each room of a modeled facility as either a small-to-moderate- L/d space or a large- L/d space, where results of future research are expected to lead to appropriate rules for such categorization. Then, when carrying out a simulation, the fire model would invoke the traditional, two-layer, isolated-plume, etc. model equations for the small-to-moderate- L/d spaces and the new model equations for large- L/d spaces.

2. Combined buoyancy- and ventilation-driven flow of a perfect gas through a long vertical shaft

Consider flow of a perfect gas through a vertical shaft of length L . Let the section of the shaft have a characteristic dimension, d , and assume that the shaft is long in the sense that $L/d \gg 1$. ρ and T , the density and temperature of the gas averaged across the section, vary along the length. In general, the shaft is ventilated; inflow or outflow of the gas can occur at vents, in the walls of the shaft, or at its ends. Inflowing gas has specified density and temperature, ρ_{VENT} and T_{VENT} , respectively, which can vary along the shaft. Outflowing gas is at density and temperature, ρ and T , respectively. The local rate of mass addition due to ventilation is \dot{m}'''_{VENT} (rate of mass added to the shaft per unit volume. Heat is transferred between the gas and the shaft surface at the rate \dot{q}'''_{HT} (rate of heat transferred to the gas in the shaft per unit volume).

Assume that the only possible significant component of flow velocity is along the axis of the shaft in the vertical z direction and let its average across a section be V_z . Then, conservation of mass and energy, and the equation of state leads to

$$\partial\rho/\partial t + \partial(V_z\rho)/\partial z = \dot{m}'''_{\text{VENT}} \quad (1)$$

$$\rho C_p(\partial T/\partial t + V_z\partial T/\partial z) = -\partial(k\partial T/\partial z)/\partial z + C_p(T_{\text{VENT}} - T)\dot{m}'''_{\text{VENT}} + \dot{q}'''_{\text{HT}} \quad (2)$$

$$\rho T = \rho_{\text{AMB}} T_{\text{AMB}} = \text{constant} \quad (3)$$

where C_p is the specific heat at constant pressure, k is the thermal conductivity, and ρ_{AMB} and T_{AMB} are the density and temperature at some ambient reference state.

Note that the formulation of Eq. (3) uses the uniformly valid assumption that variations in pressure throughout the length of the shaft are negligible compared to the characteristic pressure of the ambient reference state. At a point in the analysis where momentum considerations are required, for example in the computation of pressure differences across vents for the purpose of estimating vent flow rates, estimates of the relatively-small shaft pressure variations (e.g., the contribution of hydrostatic pressure variation) would be important and they must be estimated properly.

Using Eqs. (1) and (3) in Eq. (2) leads to the following simplified alternative to Eq. (2):

$$\partial V_z / \partial z = [-\partial(k\partial T / \partial z) / \partial z + C_p T_{\text{VENT}} \dot{m}_{\text{VENT}}''' + \dot{q}_{\text{HT}}'''] / (\rho_{\text{AMB}} T_{\text{AMB}} C_p) \quad (4)$$

3. Turbulent fluctuations in the shaft flow

3.1. The turbulence equations

Eqs. (1), (3), and (4) are now modified to account for the effect of possible turbulent fluctuations in the shaft flow. Time-averaged ('barred') and fluctuating ('primed') components of the variables are introduced:

$$\rho = \bar{\rho} + \rho', \quad T = \bar{T} + T', \quad V_z = \bar{V}_z + V'_z. \quad (5)$$

Reynolds averaging, neglect of the generally insignificant effect of heat conduction through the gas, along the length of the shaft, as derived from the time-averaged temperature distribution, and the assumption that time-averaged values of ρ and T satisfy the equation of state lead to the following modified equation set:

$$\partial \bar{\rho} / \partial t + \bar{V}_z \partial \bar{\rho} / \partial z + \partial(\bar{V}'_z \rho') / \partial z = \dot{m}_{\text{VENT}}''' (1 - \bar{\rho} / \rho_{\text{VENT}}) - (\bar{\rho} / \rho_{\text{AMB}}) \dot{q}_{\text{HT}}''' / (T_{\text{AMB}} C_p) \quad (6)$$

$$\partial \bar{V}_z / \partial z = (C_p T_{\text{VENT}} \dot{m}_{\text{VENT}}''' + \dot{q}_{\text{HT}}''') / (\rho_{\text{AMB}} T_{\text{AMB}} C_p) \quad (7)$$

$$\bar{\rho} \bar{T} = \rho_{\text{AMB}} T_{\text{AMB}} = \text{constant} \quad (8)$$

Turbulent fluctuations leading to significant values of the term $\bar{V}'_z \rho'$ in Eq. (6) will occur along the length of a vertical shaft where there are buoyancy-generated instabilities in the vertical density distribution, i.e., where, locally, the density is increasing with elevation, $\partial \bar{\rho} / \partial z > 0$. Indeed, such instabilities are the driving force for the turbulent-like mixing phenomenon which is of particular interest here. Also, shaft flow scenarios of present interest are such that \bar{V}_z is small enough as never to lead to turbulent fluctuation enhancements that would significantly affect the value of $\bar{V}'_z \rho'$. For example, at elevations along the shaft where the gas is stably stratified, i.e.,

where $\partial\bar{\rho}/\partial z \leq 0$, there will be no buoyancy-driven turbulence and it is reasonable to assume that $\partial(\overline{V'_z\rho'})/\partial z$ in Eq. (6) can be neglected completely.

Solutions to Eqs. (6)–(8) with appropriate initial and boundary conditions would generally provide a description of the fire environment that develops in ventilated, shaft-like, room configurations. However, to actually implement this equation set it is necessary to develop supplementary model equations to represent $\overline{V'_z\rho'}$ of Eq. (6) and the source terms, $\overline{m''_{\text{VENT}}}$ and $\overline{q''_{\text{HT}}}$, of Eqs. (6) and (7). The focus of the remainder of the present work is on obtaining a general representation for $\overline{V'_z\rho'}$.

3.2. Experiments in shafts with unstable density configurations: A qualitative result

During experiments in vertical tubes of diameter d , involving initially unstable configurations of saltwater over freshwater and prior to any end effects, Cannon and Zukoski [1] have observed fluid mixing by buoyancy-generated instabilities. This involved overturning and fluctuating eddies of characteristic dimension d . Also, as observed in similar unstable systems by Cannon and Zukoski [1] (heavy gas over light gas), Baird and Rice [2] (rising bubble columns), and Gardner [3] (saltwater/freshwater systems and experiments on water rising through more dense carbon tetrachloride), the propagation of buoyancy-driven turbulent fluctuations through the buoyantly unstable column behaves phenomenologically as a diffusion-like process. This is represented by the $\partial(\overline{V'_z\rho'})/\partial z$ term in Eq. (6).

3.3 A representation for $\overline{V'_z\rho'}$

3.3.1. Shaft flow systems involving negligible $\overline{V_z}$

A general representation for $\overline{V'_z\rho'}$ in Eq. (6) will now be obtained from a study of the above experiments, where compressibility and, therefore, $\overline{V_z}$ were negligible.

Consider shaft flow systems of Eqs. (6)–(8) with negligible $\overline{V_z}$ and negligible mass addition or heat transfer along the length of the shaft. For such systems, Eq. (6) becomes

$$\partial\bar{\rho}/\partial t + \partial(\overline{V'_z\rho'})/\partial z = 0 \quad (9)$$

Defining D as the eddy diffusivity for buoyancy-driven turbulence, Eq. (9), with

$$\overline{V'_z\rho'} = D\partial\bar{\rho}/\partial z \quad (10)$$

has been used in each of the above-referenced systems. It is also used by Cannon and Zukoski [1] in the modeling of a perfect gas air system, i.e. low-temperature over high-temperature air, with non-zero $\overline{q''_{\text{HT}}}$. In Eq. (10), D is expected to be an increasing function of $\partial\bar{\rho}/\partial z$ for $\partial\bar{\rho}/\partial z > 0$, and to be zero for $\partial\bar{\rho}/\partial z \leq 0$ (i.e., buoyancy-driven turbulent diffusion is suppressed at elevations where the fluid column is stably stratified).

Cannon and Zukoski [1] expect D to be proportional to w' , a characteristic velocity of the turbulent fluctuations, and to satisfy

$$D \sim w'l = [(g/\bar{\rho})\partial\bar{\rho}/\partial z]^{1/2}l^2$$

where l is a characteristic length of the fluid mixing process. Here, l is taken to be the characteristic dimension of the observed buoyancy-driven eddies, namely, d .

$$D = \begin{cases} Kd^2 [(g/\bar{\rho})\partial\bar{\rho}/\partial z]^{1/2} & \text{if } \partial\bar{\rho}/\partial z > 0 \\ 0 & \text{if } \partial\bar{\rho}/\partial z \leq 0 \end{cases} \quad (11)$$

where K is a constant and where a version of Eq. (11) is also found in Refs. [2, 3].

3.3.2. A determination of K ; a steady-state experiment

To determine K , Gardner [3] considered the particular problem of quasi-steady turbulent diffusion in a long vertical shaft connecting two relatively large vessels of incompressible fluids, with density of the fluid in the top and bottom vessels, ρ_{TOP} and $\rho_{\text{BOT}} < \rho_{\text{TOP}}$, respectively, where $\Delta\rho = \rho_{\text{TOP}} - \rho_{\text{BOT}}$ is such that $\Delta\rho/(\rho_{\text{TOP}} + \rho_{\text{BOT}}) \ll 1$. To insure that $V_z = 0$, at least one of the vessels is fully enclosed. This problem was studied experimentally by Mercer and Thompson [4] with saltwater/freshwater systems and circular shafts of diameter, d .

For the above class of problem, $\bar{\rho} \approx \rho_{\text{AVE}} = (\rho_{\text{TOP}} + \rho_{\text{BOT}})/2$ and

$$D \approx Kd^2 [(g\Delta\rho/\rho_{\text{AVE}})dc_{\text{TOP}}/dz]^{1/2}; \quad -Ddc_{\text{BOT}}/dz = Ddc_{\text{TOP}}/dz \quad (12)$$

where Q is the volume flow rate of the fluid in the lower vessel diffusing up through the shaft and into the top vessel and where c_{TOP} , c_{BOT} are the concentrations in the shaft of the top and bottom fluids, respectively.

With quasi-steady systems of saltwater over freshwater, Mercer and Thompson [4] determined Q of freshwater from the lower vessel by measuring salt concentrations and the rates of mass decrease of the salt water in a top vessel. Using their vertical shaft results in Eqs. (12), Gardner [3] determined

$$K = K_G = 0.56 \quad (13)$$

In contrast to this, Baird and Rice [2] analyzed the literature on rising bubble columns and related systems where gas flow rates are large enough for the bubble wakes to interact strongly and to generate turbulence in the opposing fluid motion. For such systems they determined the 'order-of-magnitude estimate'

$$K = K_{\text{BR}} = 0.21 \quad (14)$$

4. Unsteady experiments to verify Eqs. (9)–(11) and the value of K

4.1. Description of the two-phase experiments

The unsteady experiments of Cannon and Zukoski [1] included the configuration of Fig. 2 involving a tube of length L , closed at the upper end, $z = L$, and inserted into

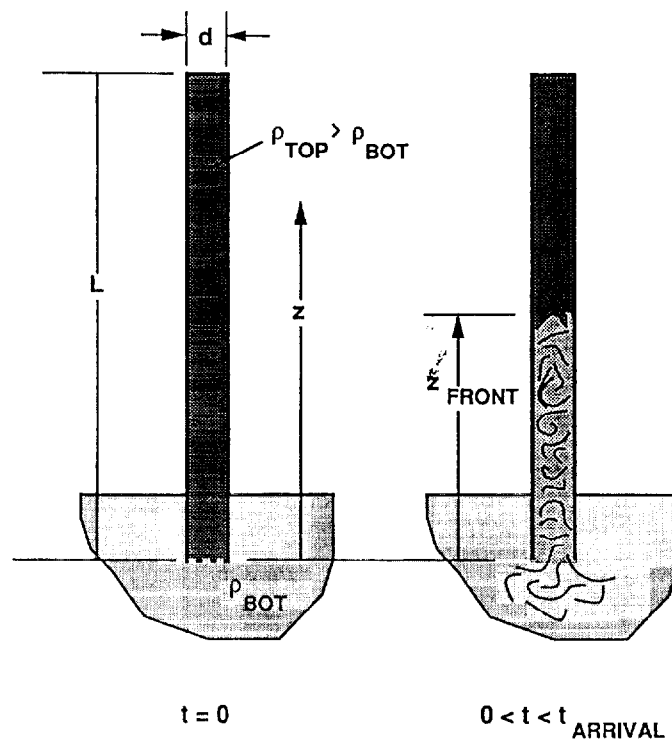


Fig. 2. Sketch of the simulated experiments of Cannon and Zukoski [1].

a relatively large vessel of density ρ_{BOT} . The tube was initially filled with fluid of density $\rho_{\text{TOP}} > \rho_{\text{BOT}}$. The experiments were initiated by allowing the fluid in the tube to mix with the fluid in the lower vessel. The mixing involves two phases, Phases I and II. Phase I begins when the experiment is initiated. A diffusion front at $z = z_{\text{FRONT}}(t)$, $z_{\text{FRONT}}(0) = 0$, rises and in $0 \leq z \leq z_{\text{FRONT}}(t)$ there is mixing due to non-zero $\partial \bar{\rho} / \partial z$. Phase I is completed and Phase II is initiated at $t = t_{\text{ARRIVAL}}$, when $z_{\text{FRONT}} = L$, i.e., at the time of arrival at the top of the tube of the diffusion front, when the effects of the diffusive mixing begin to modify the density at the upper end of the tube. During the remainder of Phase II, for $t > t_{\text{FRONT}}$, the unstable density distribution drives turbulent-like mixing eddies through the length of the tube. The distribution eventually relaxes to the uniform state, $\rho = \rho_{\text{BOT}}$.

Data from both Phases I and II of the Cannon and Zukoski experiments [1] can be used to verify the model Eqs. (9)–(11) and the value of K . The next section addresses the Phase I phenomena.

4.2. The initial value problem for the diffusion front: Phase I

4.2.1. Problem formulation and similarity

From Eqs. (9)–(11), the initial value problem for Phase I is

$$\frac{\partial \theta}{\partial \tau} = \frac{\partial}{\partial \zeta} \left[\frac{1}{(1 + \varepsilon \theta)^{1/2}} \left(\frac{\partial \theta}{\partial \zeta} \right)^{3/2} \right], \quad (15)$$

$$\theta(\zeta = 0, \tau > 0; \varepsilon) = 0; \quad \frac{\partial \theta}{\partial \zeta}(\theta = 1) = \frac{\partial \theta}{\partial \zeta}(\tau = \tau_{\text{FRONT}}, \zeta = \zeta_{\text{FRONT}}; \varepsilon) = 0, \quad (16)$$

$$\theta = \frac{(\bar{\rho} - \rho_{\text{BOT}})}{(\rho_{\text{TOP}} - \rho_{\text{BOT}})}; \quad \zeta \equiv z/d; \quad \tau \equiv K[\varepsilon d/d]^{1/2}t; \quad \varepsilon \equiv \Delta\rho/\rho_{\text{BOT}} \quad (17)$$

Note that Eqs. (15)–(17) specify $\bar{\rho}(z = 0) = \rho_{\text{BOT}}$. However, as discussed by Cannon and Zukoski [1], $\bar{\rho}$ at the base of the tube will always be somewhat greater than ρ_{BOT} , i.e., $\theta(\zeta = 0; \tau > 0) = \delta(\tau)$ where δ presumably satisfies $0 < \delta \ll 1$. Thus, the indicated boundary condition, $\theta(\zeta = 0; \tau > 0) = 0$, of Eq. (16) is only approximately correct. In particular, the solution to Eqs. (15)–(17) can be expected to provide a good simulation of experimental values only for moderate-to-large values of ζ and ζ_{FRONT} .

Introducing the similarity variable η , it can be shown that

$$\theta = \theta(\eta; \varepsilon) \quad \text{where } \eta = \zeta/\tau^{2/5} \quad (18)$$

and that the problem of Eqs. (15)–(17) can be reduced to

$$\eta \frac{d\theta}{d\eta} = -\frac{5}{2} \frac{d}{d\eta} \left[\frac{1}{(1 + \varepsilon\theta)^{1/2}} \left(\frac{d\theta}{d\eta} \right)^{3/2} \right], \quad 0 \leq \theta \leq 1; \quad (19)$$

$$\theta(\eta = 0) = 0; \quad \frac{d\theta}{d\eta}(\theta = 1) = \frac{d\theta}{d\eta}(\eta = \eta_{\text{FRONT}}) = 0; \quad \eta_{\text{FRONT}} = \eta_{\text{FRONT}}(\varepsilon)$$

where η_{FRONT} is the smallest value of η satisfying the above condition.

Once Eqs. (19) are solved, the position of the front, $\eta_{\text{FRONT}}(\varepsilon)$, can be determined from

$$\zeta_{\text{FRONT}}(t; \varepsilon) = z_{\text{FRONT}}(t; \varepsilon)/d = \eta_{\text{FRONT}}(\varepsilon)[K(\varepsilon g/d)^{1/2}t]^{2/5} \quad (20)$$

4.2.2 Solution for small ε : verification with saltwater/freshwater experiments

For the saltwater/freshwater experiments of Cannon and Zukoski [1], ε always satisfies $\varepsilon < 0.2$. Therefore, the $\varepsilon = 0$ solution of Eqs. (15)–(17) should provide a good simulation. This solution is found to be

$$\theta(\eta; \varepsilon = 0) = \frac{3}{8} \left(\frac{\eta}{\eta_{\text{FRONT}}} \right) \left[\left(\frac{\eta}{\eta_{\text{FRONT}}} \right)^4 - \frac{10}{3} \left(\frac{\eta}{\eta_{\text{FRONT}}} \right)^2 + 5 \right], \quad 0 \leq \frac{\eta}{\eta_{\text{FRONT}}} \leq 1 \quad (21)$$

$$\eta_{\text{FRONT}} = \eta_{\text{FRONT}}(\varepsilon = 0) = 15^{3/5}/8^{1/5} = 3.3499\dots$$

$$\zeta_{\text{FRONT}}(t; 0 < \varepsilon \ll 1) = z_{\text{FRONT}}(t; 0 < \varepsilon \ll 1)/d = (15^{3/5}/8^{1/5})[K(\varepsilon g/d)^{1/2}t]^{2/5} \quad (22)$$

Eq. (22) is plotted in Fig. 3 for the K 's of Eqs. (13) and (14). (The $K = 0.438$ plot will be explained below in the discussion of Phase II.)

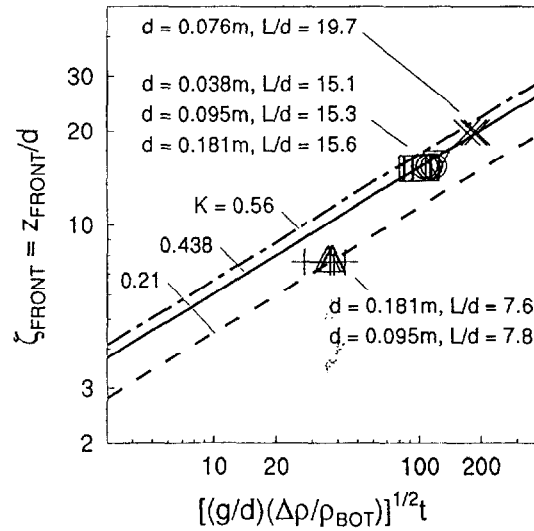


Fig. 3. Position of the diffusion front in Phase I: small- ε solution of Eq. (22) for different values of K ; and values measured in the saltwater/freshwater experiments of Cannon and Zukoski [1].

The saltwater/freshwater experiments of Cannon and Zukoski [1] cover the d , L/d range $0.030 \text{ m} \leq d \leq 0.181 \text{ m}$, $7.6 \leq L/d \leq 40.3$. For many, but not all of these experiments they tabulate (Table 6-2 of [1]) and/or plot (Figure 6.13 of [1]) t_{ARRIVAL} . These data are included in Fig. 3. In the figure, note that when K is taken to be $K_G = 0.56$ the larger values of the ζ_{FRONT} data are well-predicted by Eq. (22). (Recall that this value of K was also deduced from experiments in a saltwater/freshwater system.) It is also noteworthy that t_{ARRIVAL} data for the largest L/d experiments $L/d = 29.3$ and 40.3 , are not reported in [1] and, therefore, are not included in Fig. 3. However, data from these experiments up to $\zeta_{\text{FRONT}} \approx 25$ are reported. For times prior to t_{ARRIVAL} , the $K = 0.56$ plot of Fig. 3 continues to predict well this data. Also, because of the aforementioned approximate nature of the $\eta = 0$ boundary condition of Eqs. (19), and because the characteristic d -dimension of the turbulent-like eddies are associated with ζ intervals of the order of 1, small-to-moderate values of ζ_{FRONT} are not expected to be well-simulated by the Eq. (22) solution.

4.2.3. Solution for moderate-to-large ε ; verification with heavy-gas/light-gas experiments

Simulations of the Cannon and Zukoski [1] heavy-gas/light-gas experiments require solutions to Eqs. (19) with moderate-to-large values of ε . To study these, it is convenient to solve an alternative set of equations for θ , ψ , and ϕ :

$$\begin{aligned} \frac{d\phi}{d\eta} &= -\left(\frac{4}{15}\right)\eta\phi^{1/2}(1+\varepsilon\theta)^{1/2} + \left(\frac{\varepsilon}{3}\right)\frac{\phi^2}{(1+\varepsilon\theta)} \\ \frac{d\psi}{d\eta} &= \theta; \quad \frac{d\theta}{d\eta} = \phi, \quad 0 \leq \theta \leq 1 \quad \text{where } \theta(\eta=0) = \psi(\eta=0) = 0 \end{aligned} \quad (23)$$

and where $\Gamma(\varepsilon) = \phi(\eta=0) = d\theta/d\eta(\eta=0)$ is determined such that

$$\theta = 1; \quad \phi = d\theta/d\eta = 0 \quad \text{at some minimum } \eta = \eta_{\text{FRONT}}(\varepsilon).$$

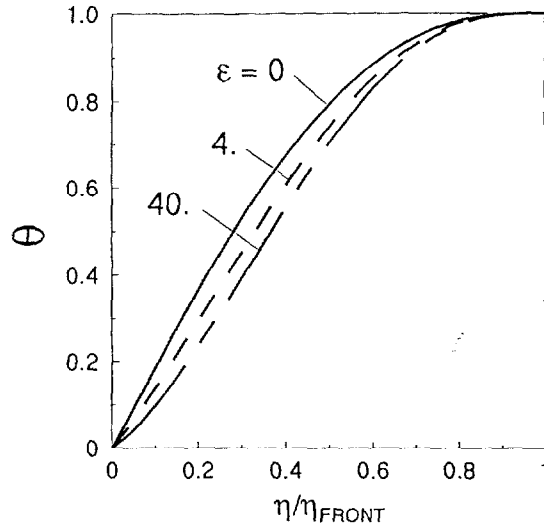


Fig. 4. Phase I solution of Eqs. (23) for $\theta(\eta/\eta_{FRONT}; \epsilon)$ including moderate-to-large ϵ .

Solutions for ψ will be used below in the Phase II analysis:

$$\psi(\eta; \epsilon) = \int_0^\eta \theta(\omega; \epsilon) d\omega \tag{24}$$

Numerical integration of Eqs. (23) was carried out. This yielded $\theta(\eta; \epsilon)$, $\Gamma(\epsilon)$, $\eta_{FRONT}(\epsilon)$, and $\psi(\eta; \epsilon)$ for $0 < \epsilon \leq 40$. Results for $\theta(\eta; \epsilon)$, including the $\theta(\eta; \epsilon = 0)$ result of Eq. (21) are plotted in Fig. 4. As can be seen, $\theta(\eta/\eta_{FRONT}; \epsilon)$ is relatively insensitive to differences in ϵ . The reader is referred to Fig. 4b–d of References [5] for plots of $\Gamma(\epsilon)$, $\eta_{FRONT}(\epsilon)$, and $\psi(\eta; \epsilon)$, respectively.

Cannon and Zukoski [1] carry out heavy-gas/light-gas experiments with $d = 0.152$ m, $L/d = 12$, $\epsilon = 0.22, 0.38$, and 4.0 . Fig. 6.14 of [1] presents Phase II data on $\theta(\zeta = L/d, \tau > \tau_{ARRIVAL}; \epsilon, L/d)$. However, Phase I data for these experiments are not provided. Also, note that estimates of $t_{ARRIVAL}$ by extrapolation of the Phase II data to $\theta = 1$ are subject to significant error because increases in ϵ lead to decreases in $t_{ARRIVAL}$ [e.g., $t_{ARRIVAL}$ is estimated from Eq. (26) to be of the order of 5 s when $\epsilon = 4.0$], and because of the ‘slow response time of the system used to measure the density of the gas mixture [1]’.

4.3. Relaxation of the diffusion front: Phase II

4.3.1. The initial value problem for Phase II

Subsequent to $t = t_{ARRIVAL}$, θ is no longer characterized by the similarity variable. Rather, it must be determined from a solution of Eq. (15) subject to

$$\theta(\zeta = 0, \tau > \tau_{ARRIVAL}; \epsilon) = \frac{\partial \theta}{\partial \zeta}(\zeta = L/d, \tau > \tau_{ARRIVAL}; \epsilon) = 0 \tag{25}$$

$$\theta(\zeta, \tau = \tau_{ARRIVAL}; \epsilon) \equiv Z(\zeta; \epsilon) = \theta(\eta = \zeta/\tau_{ARRIVAL}^{2/5}; \epsilon) \tag{26}$$

$$\tau_{ARRIVAL} \equiv K[\epsilon g/d]^{1/2} t_{ARRIVAL} = [(L/d)/\eta_{FRONT}(\epsilon)]^{5/2}$$

4.3.2. An approximation solution

Partial verification of Eqs. (9)–(11) during Phase II can be obtained by an integral-type approximate solution to Eqs. (15) and (25). Toward this end, Eq. (15) is first integrated in ζ in the interval $0 \leq \zeta \leq L/d$. Using the boundary conditions of Eqs. (25), this leads to

$$\frac{d}{d\tau} \left[\int_0^{L/d} \theta(\zeta, \tau; \varepsilon) d\zeta \right] = - \left(\frac{d\theta}{d\zeta} \Big|_{\zeta=0} \right)^{3/2} \quad (27)$$

Now choose the following approximate solution form, which satisfies exactly Eqs. (25):

$$\theta = \theta(\zeta, \tau = \tau_{\text{ARRIVAL}}; \varepsilon) T(\tau; \varepsilon, L/d); T(\tau = \tau_{\text{ARRIVAL}}; \varepsilon, L/d) = 1 \quad (28)$$

Using Eq. (28) in Eq. (27) eventually leads to

$$T(\tau; \varepsilon, L/d) = \{ [\Omega(\varepsilon)/(L/d)^{5/2}] (\tau - \tau_{\text{ARRIVAL}}) + 1 \}^{-2} \quad (29)$$

$$\Omega(\varepsilon) = [\eta_{\text{FRONT}}^{5/2}(\varepsilon) \Gamma^{3/2}(\varepsilon/2)] / \psi[\eta_{\text{FRONT}}(\varepsilon); \varepsilon]$$

where $\Omega(\varepsilon)$ is plotted in Fig. 5.

4.3.3. Solution for small ε ; saltwater/freshwater experiments

Eqs. (21), (22), and (29) lead to

$$\Omega(\varepsilon = 0) = (15^{3/2}/2^{1/2})/11 = 1.8672\dots \quad (30)$$

Using Eqs. (28)–(30), the Phase II solution at $z = L$ for $\varepsilon \rightarrow 0$ and $L/d = 15.3$ is plotted in Fig. 6. This solution would be used to simulate the saltwater/freshwater experiments of Cannon and Zukoski [1]. Phase II data from these are presented in Fig. 6.9

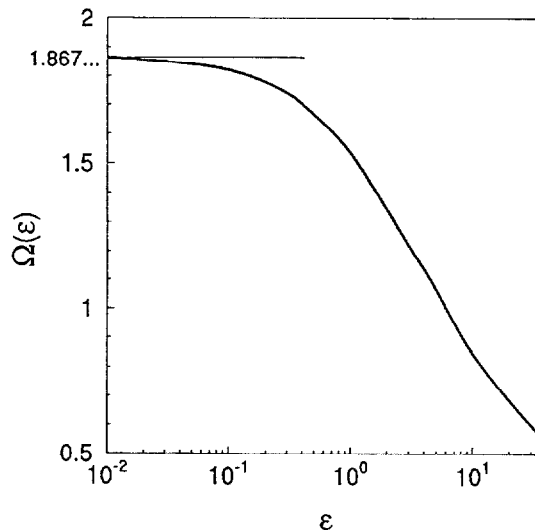


Fig. 5. Plot of $\Omega(\varepsilon)$ of Eq. (29) from Phase II solutions of Eqs. (27) and (28).

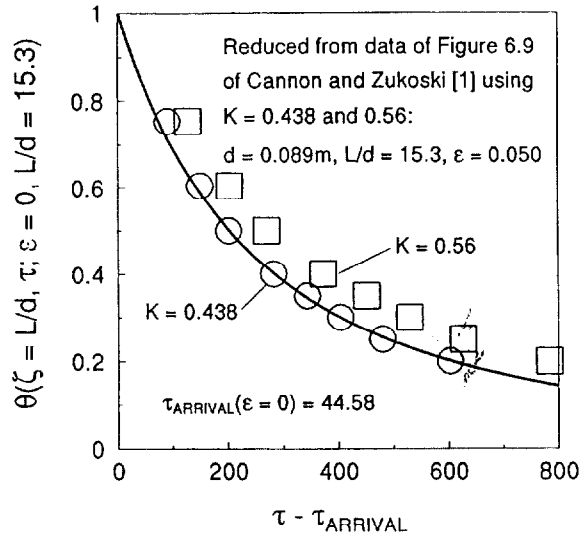


Fig. 6. Plots for Phase II: Eqs. (28)–(29) at $z = L$ for $\varepsilon = 0$; slatwater/freshwater data of Cannon and Zukoski [1] using $K = 0.56$ and least-squares-fit value $K = 0.438$.

of [1] for $d = 0.089$ m, $L/d = 15.3$, $\varepsilon = 0.050$. Reducing these data for plotting in Fig. 6 requires K . Two values were used, and corresponding reduced data sets were obtained and plotted. The first is $K = K_G = 0.56$. The second is that value of K which provides the least-squares fit between the data and the theoretical solution. The latter value was found to be $K = 0.438$, and, as seen in the figure, this provides an excellent match between theory and experiment during Phase II.

Using the ‘best-fit’ $K = 0.438$, a plot of the corresponding, theoretical, Phase I-solution has also been included in Fig. 3. As can be seen, this value of K and the corresponding solution provides a somewhat better match to the Phase I data than does that of the $K = 0.56$ solution.

4.3.4. Solutions for moderate ε : heavy-gas/light-gas experiments

Using Eqs. (28)–(29), the Phase II solutions at $z = L$ for $\varepsilon = 0.22$, 0.38 , and 4.0 are plotted in Fig. 7. These approximate solutions are to be compared to the heavy-gas/light-gas data of Fig. 6.14 of Cannon and Zukoski [1]. Again, reduction of the data requires K . This is chosen to be the previously determined ‘best-fit’ value, $K = 0.438$. As can be seen, the comparison between theory and experiment is good, especially for $\varepsilon = 0.22$ and 0.38 .

5. Summary, conclusions, and recommendations

A limitation of zone-type compartment fire models is the lack of a satisfactory means of simulating time-dependent fire-generated environments in ventilated shaft-like spaces with large height-to-span (L/d) ratios. For such configurations, the

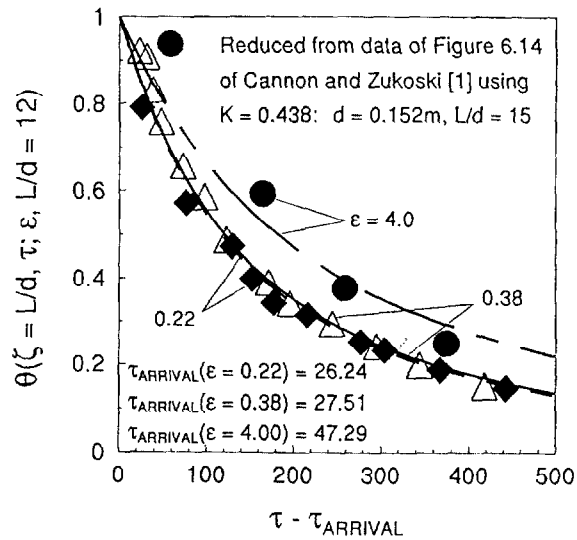


Fig. 7. Plots for Phase II: Eqs. (28)–(29) at $z = L$ for $\epsilon = 0.22, 0.38,$ and 4.0 ; heavy-gas/light-gas data of Cannon and Zukoski [1] using $\epsilon = 0.22, 0.38,$ and 4.0 using $K = 0.438$.

traditional two-layer zone-model-type description of a room fire environment is not valid. Experiments reported in the literature suggest that the environment be modeled as a time- and elevation-dependent density distribution, where intervals of instability (i.e., density increasing with elevation) are removed by the action of overturning and fluctuating turbulent-like mixing eddies of characteristic dimension, d , and where the mixing phenomenon has the features of a diffusion-like process.

Consistent with the above ideas, a general set of model equations, Eqs. (6)–(8), (10) and (11), was developed to simulate combined buoyancy-and ventilation-driven flow through long vertical shafts. Required to implement this equation set was a universal constant K , the coefficient of a turbulent diffusivity term that leads to modifications in density distribution in regions where the unstable density distribution prevails.

Solutions were obtained for a special class of problem that isolates K and the turbulent diffusivity term and that involves no net ventilation flow and no wall-to-gas heat transfer. The result, $K = 0.44$, was then obtained by using the solutions to correlate data from unsteady (Fig. 2) type saltwater/freshwater experiments of Cannon and Zukoski [1]. With this value, addition data from [1] for both saltwater/freshwater and heavy-gas/light-gas experiments were shown to be well-simulated by the new model equation set.

Based on the above, it is recommended that the model equation set, with $K = 0.44$, be used in room fire models to describe the development of fire environments in ventilated, shaft-like, room configurations. This model formulation will require further development of the heat transfer term of Eqs. (6) and (7), i.e., a verified method of simulating \dot{q}''_{HT} . Also, the model equations will be subject to verification with data from experiments on hot-air/cold-air systems, including fire-driven smoke flows, which involve gas-to-surface heat transfer exchanges.

References

- [1] Cannon JB, Zukoski EE. Turbulent mixing in vertical shafts under conditions applicable to fires in high rise buildings. Tech. Report 1 of California Institute of Technology under NSF Grant G131892X, January 1976.
- [2] Baird MHI, Rice RG. Axial dispersion in large unbaffled columns. *Chem Engng*, 1975; 9:171.
- [3] Gardner GC. Motion of miscible and immiscible fluids in closed horizontal and vertical ducts. *Int J Multiphase Flow*, 1977;3:305.
- [4] Mercer A, Thompson H. An experimental investigation of some further aspects of the buoyancy-driven exchange flow between carbon dioxide and air following a depressurization accident in a Magnox reactor. *J Brit Nucl Energy Soc*, 1975;14:327.
- [5] Cooper LY. Simulating smoke movement through long vertical shafts in zone-type compartment fire models. NISTIR 5526, U.S. National Institute of Standards and Technology, Gaithersburg MD, 1994.